Growth Velocity and Direct Length-Sorted Growth of Short Single-Walled Carbon Nanotubes by a Metal-Catalyst-Free Chemical Vapor Deposition Process

Bilu Liu,[†] Wencai Ren,*[,†] Chang Liu,[†] Cheng-Hua Sun,[‡,§] Libo Gao,[†] Shisheng Li,[†] Chuanbin Jiang,[†] and Hui-Ming Cheng*[,†]

[†]Shenyang National Laboratory for Materials Science, Institute of Metal Research, Chinese Academy of Sciences, Shenyang 110016, P. R. China, [‡]ARC Center of Excellence for Functional Nanomaterials, School of Engineering and Australian Institute of Bioengineering and Nanotechnology, The University of Queensland, QLD 4072, Australia, and [§]Center for Computational Molecular Science, Australian Institute for Bioengineering and Nanotechnology, The University of Queensland, QLD 4072, Australia

ABSTRACT We report on the observation of a very low growth velocity of single-walled carbon nanotubes (SWNTs) and consequently the direct length-sorted growth and patterned growth of SWNTs by using a metal-catalyst-free chemical vapor deposition (CVD) process proposed recently by our group, in which SiO_2 serves as catalyst. We found that the growth velocity of the SWNTs from SiO_2 catalyst is only 8.3 nm/s, which is about 300 times slower than that of the commonly used iron group catalysts (Co as a counterpart catalyst in this study). Such a slow growth velocity renders direct length-sorted growth of SWNTs, especially for short SWNTs with hundreds of nanometers in length. By simply adjusting the growth duration, SWNTs with average lengths of 149, 342, and 483 nm were selectively obtained and SWNTs as short as ~20 nm in length can be grown directly. Moreover, comparative studies indicate that the SiO_2 catalyst possesses a much longer catalytic active time, showing sharp contrast with the commonly used Co catalyst which quickly loses its catalytic activity. Taking advantage of the very slow growth velocity of the SiO_2 catalyst, patterned growth of SWNT networks confined in a narrow region of <5 μm was also achieved. The short SWNTs may show intriguing physics owing to their finite length effect and are attractive for various practical applications.

KEYWORDS: carbon nanotubes · length · metal-catalyst-free · growth velocity · catalyst activity · patterned growth

Single-walled carbon nanotubes (SWNTs) have attracted intense research interest owing to their exceptional electrical, optical, thermal, and mechanical properties. The electronic properties of SWNTs depend sensitively on their geometry structure, that is, diameter and chirality.[1] Many practical applications demand SWNT species with particular structures and properties; for example, semiconducting SWNTs can be used for fabricating field effect transistors (FETs),[2] while metallic SWNTs are desirable in making transparent conductive films (TCFs).[3] Considerable efforts have thus been made recently toward controlling the diameter and chirality of SWNTs, both through selective growth approach[4−8] and postseparation/enrichment.[9−11]

The length of SWNTs, on the other hand, is another very important factor which determines the physical properties of SWNTs.[12−16] The length-dependent properties, such as electronic and electrical transport properties,[1,14−18] dielectric polarization,[19] optical properties,[14] thermal conductivity,[1,13,20] carrier recombination,[12] and pathogenicity[21] have been theoretically predicted[13,17] and some of them experimentally validated.[1,14,16,18−20] For example, scanning tunneling microscope and spectroscopy (STM/STS) studies revealed the large energy level splitting in short (cut down to 30 nm) metallic SWNTs,[18] and ballistic transport through short SWNTs (300 nm in length), beneficial from free acoustic phonon scattering,[1,15,16] is also demonstrated, which is attractive for fabrication of memory and logic devices.[15] Very recently, a blue shift in electronic transitions between van Hove singularities for short surfactant encapsulated SWNTs with length down to several nanometers, named SWNT quantum dots, has also been observed.[22] More importantly, some practical applications of SWNTs are unique length required (*e.g.*, in electronic devices, sensors) and short length preferred, such as scanning probes,[12,23,24] catalyst supports,[25] biological imaging,[26,27] molecular sensing,[26] electronic devices,[26,28] *etc.* With the increase in the density of integration of SWNT-based electronics, the length of SWNTs used in electronic devices is approaching submicrometer to even nanometer scales.[19]

*Address correspondence to cheng@imr.ac.cn, wcren@imr.ac.cn.

Received for review July 14, 2009 and accepted October 18, 2009.

Published online October 26, 2009.
10.1021/nn900799v CCC: $40.75

However, compared to the exploration on the diameter and chirality control of SWNTs, very few efforts have been devoted toward length-selected preparation of SWNTs, especially for short SWNTs.[22] Moreover, all the current established approaches for the preparation of short SWNTs, such as mechanical milling and cutting,[27,29,30] high-power sonication,[21,22,31] and chemical cutting,[28,32−34] are post-treatment methods in the framework of top-down strategy. Those processes inevitably introduce defects to SWNTs, such as structural defects on tube walls (*e.g.*, the disruption of tubular structure,[30] "worm-eaten" like damage,[27] and Stone−Wales defects), opened ends,[21,22,29,31] and chemical functionalization.[33,34] The obtained short SWNTs are also simultaneously contaminated by abrasive materials employed in some processes,[27−29] and the use of chemicals and surfactants inhibits the intrinsic property characterization of SWNTs due to their reaction and interaction.[35,36] Other approaches, such as voltage pulse induced cutting, are only suitable for individual nanotube level.[18]

To the best of our knowledge, there are very few reports on direct length-sorted growth of SWNTs, namely, bottom-up strategy, especially for short SWNTs down to hundreds of nanometers.[37] One of the major obstacles for the selective growth of short SWNTs is that the growth velocity of SWNTs is usually very fast for the commonly used iron group catalysts based on chemical vapor deposition (CVD) process (which will be discussed later), and consequently, the growth process runs in a plausible "uncontrollable" way. Thus, it is difficult to control the length of SWNTs even in a micrometer range.

From the reaction point of view, the growth velocity of SWNTs is mainly dependent on the following steps: (i) carbon source dissociation, (ii) carbon atom diffusion through the catalyst, and (iii) carbon atom incorporation into SWNT wall.[38,39] It is important to note that the former two steps should be strongly related to the properties of catalyst (*e.g.*, its structure, composition, and melting point),[38,40] and catalyst is thus one of the key factors which can remarkably influence the reaction kinetics of SWNT growth. The third step, as will be discussed later, is not the growth velocity-limiting step. Therefore, developing new catalysts should be a rational and efficient avenue toward slowing down the reaction and realizing the length control of SWNTs by a direct growth approach.

Very recently, we developed a metal-catalyst-free CVD process for the growth of high quality SWNTs, in which a 30-nm-thick sputtering deposited SiO_2 film served as catalyst,[41,42] which was also reported by Huang's group.[43] Since SiO_2 is chemically inert and its function of catalytically decomposing hydrocarbons is very limited, it is reasonable to expect that the step (i) abovementioned, that is, the carbon source dissociation, is remarkably slowed down in this case, which will accordingly slow down the whole growth process and fulfill direct growth of short SWNTs. In this contribution, by further studying the growth kinetics of SWNTs from SiO_2 catalyst, we found that this catalyst system indeed has an extremely slow growth velocity of 8.3 nm/s in our growth conditions, about 300 times smaller than that of the commonly used iron group catalysts (Co catalyst was used in this study for comparative studies). The slow growth velocity provides an efficient means toward direct length-sorted growth of SWNTs with average lengths down to 149 nm, and the shortest SWNTs of ~20 nm in length can be directly grown. Benefiting from the slow growth velocity of the SiO_2 catalyst, we also demonstrated that the SiO_2 film deposition process can be easily integrated for the patterned growth of SWNT networks where SWNTs can be well restricted in a narrow region. Moreover, we found that the SiO_2 based catalyst keeps active during the whole 20 min growth process, showing sharp contrast with the iron group catalysts that easily lose their catalytic activity within several minutes.

RESULTS AND DISCUSSION

Slow Growth Velocity. The CVD growth process is similar to our previous communication[41] and the details are described in the experimental section. In brief, 30-nm-thick SiO_2 film deposited SiO_2/Si wafers were employed as substrates and the SWNT growth was performed at 900 °C using CH_4 as carbon source. Our previous communication confirmed the formation of abundant nanoparticles (NPs) after pretreatment of the deposited SiO_2 film, which serves as the catalyst for SWNT growth.[41] To investigate the reaction kinetics of the SWNTs grown from SiO_2 catalyst, we first studied the length increase of the SWNTs through tuning the growth time within 60 s. To precisely control the growth duration, two means were applied to guarantee a prompt termination of the growth: (i) flushing the residual CH_4 gas with a large flow of Ar + H_2 gas mixture[44] and (ii) pulling out the reaction tube from high temperature area just after the growth. Figure 1 panels a, b, and c show atomic force microscopy (AFM) images of the SWNTs with a growth time duration of 20, 40, and 60 s, respectively. The corresponding length distribution plots are presented in the right panels for each image. Gaussian fitting suggests the SWNT average lengths (L) of 149, 342, and 483 nm for the 20, 40, and 60 s grown samples, respectively, and also presented in each plot are the standard deviation (sd) and the number of SWNTs (N) for the statistic analysis. The length distributions also suggest that most of the SWNTs are well confined in a narrow length range; that is, 78.0% (64 in 82) of SWNTs in Figure 1a has length ≤ 250 nm; for Figure 1b, 92.5% (99 in 107) has length ≤ 600 nm; for Figure 1c, 85.8% (109 in 127) has length ≤ 1100 nm. Careful inspections reveal that both the average length and the shorter-length side tail of the SWNTs are

increased upon prolonging the growth duration. For example, for the 40 s growth sample, 27.1% (29 in 107) SWNTs have length ≤250 nm; while the 60 s growth sample shows only 9.4% (12 in 127) SWNTs shorter than 250 nm. We also note that there are indeed some very short nanotubes, although only a few, with lengths far less than the mean length of the sample, such as SWNTs with lengths of ~100 nm for the 1 min growth sample. This might be caused by the asynchronous nucleation and growth of SWNTs among different catalyst NPs, that is, not all the SWNT growth took place at the exact same time.[44] The shortest SWNT, observed in Figure 1a, is only ~20 nm, which approaches the resolution limitation of the AFM tip used in this study. The direct length-sorted growth of SWNTs, especially short SWNTs with average length of 149 nm, has not been reported and is important for some intrinsic properties investigation of SWNTs.

The above obtained length data suggest that the growth velocity of SWNTs in this process is very slow. According to the formula $v = L/t$, where v is the growth velocity of SWNTs (nm/s), and L is the length of the SWNT grown (nm) during the growth duration, t (s), we can calculate the average growth velocity of the SWNTs with growth durations of 20, 40, and 60 s. As shown in Figure 2, linear fitting of these three data gives a growth velocity of 8.3 nm/s. There are a very small portion of SWNTs with length much longer than the corresponding average length for each period of growth time, such as the SWNT with a length of ~1.45 μm for 20 s growth sample. Nevertheless, even for this longest nanotube, a slow growth velocity of ~73 nm/s was obtained. Considering the fact that most of the as grown SWNTs are well confined in a narrow region around the average length for each period of growth duration, it is reasonable to believe that the average growth velocity presented above represents the typical growth behavior of SWNTs from SiO_2 catalyst in our process.

It is surprising to note that this velocity is significantly smaller than that of SWNTs catalyzed by the commonly used Fe, Co, and Ni catalysts.[45−48] Despite the slight difference in the growth velocity and the inconsistency of velocity trends among these catalysts reported by different groups, the typical growth velocity of these three catalysts is similar, having a value of several micrometers per second. For instance, 20 μm/s was reported by Huang *et al.* in CH_4−FeMo system,[45] ~4.5 to 22.4 μm/s was reported by Yao *et al.* in an ethanol−Fe system[46] for the growth of horizontally aligned SWNTs, and ~4.2 μm/s was reported by Hata *et al.* in C_2H_4−Fe or Co system for the growth of vertical SWNT forests,[49] as summarized in Table 1. The growth velocity of 8.3 nm/s is also significantly smaller than that of random networks of SWNTs grown on substrates by using iron group catalysts, such as the data reported by Reina *et al.*,[44] where Fe (derived from $FeCl_3$ or ferritin as precursor) was used as catalyst and giving an average growth velocity of >200 nm/s (as can be discerned from Figure 2e of the reference).

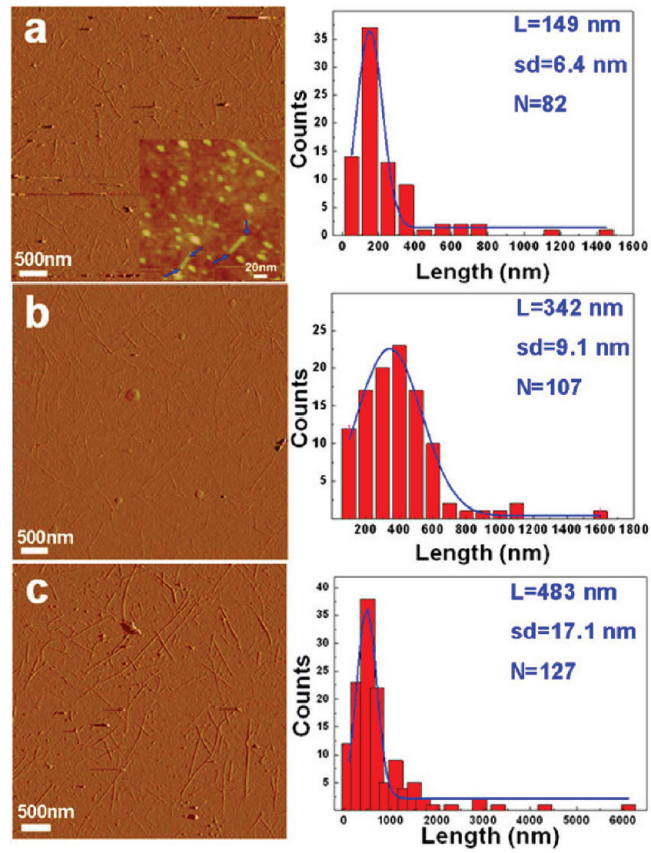

Figure 1. Amplitude AFM images of the short SWNTs grown on SiO_2/Si substrates, with growth durations of 20 s (a), 40 s (b), and 60 s (c). The right panels are the corresponding SWNT length distribution, where Gaussian fitting suggests average lengths L (standard deviation, sd) of 150 (6.4), 342 (9.1), and 483 nm (17.1 nm) for the 20, 40, and 60 s growth samples, respectively. The N in each plot is the number of SWNTs for the statistic analysis. The inset in image a is a zoom-in height mode AFM image of two short SWNTs (indicated by blue arrows), with lengths (diameters) of ~22 (1.2) and 34 nm (1.4 nm).

Note that in some of the above previous studies, CH_4 was also applied as carbon source (the same as

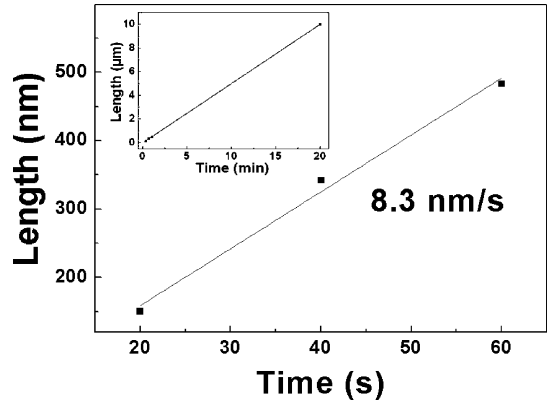

Figure 2. Growth velocity of the SWNTs from SiO_2 catalyst. Linear fitting of the 20, 40, and 60 s growth data suggests an average growth velocity of 8.3 nm/s. Inset is an extended fitting line, giving a SWNT length of ~10 μm for 20 min growth time.

TABLE 1. Summary of the Growth Velocities of SWNTs

carbon source	catalyst	SWNT type	growth velocity	refs
CH_4	FeMo	horizontally aligned	20 μm/s	Huang *et al.*[45]
C_2H_5OH	Fe	horizontally aligned	4.5−22.4 μm/s	Yao *et al.*[46]
C_2H_4	Fe or Co	vertically aligned	4.2 μm/s	Hata *et al.*[49]
CH_4 or C_2H_5OH	Fe	horizontally aligned	2 μm/s	Reina *et al.*[44]
CH_4 or C_2H_5OH	Fe	random network	>200 nm/s	Reina *et al.*[44]
CH_4	SiO_2	random network	8.3 nm/s	this work
CH_4	Co	random network	~2.5 μm/s	this work

our case).[44,45] This fact indicates that the different growth velocities may originate from the intrinsic difference between catalysts, that is, SiO_2 *versus* traditional iron group catalysts. However, it is reasonable to expect that the growth velocity of SWNTs should be strongly dependent on the growth temperature, carbon source type and its concentration, and reaction conditions.[38,43−47,50−53] To further eliminate these influences and make a precise comparison, we performed SWNT synthesis using a commonly used Co catalyst, where the Co catalyst NPs were synthesized *via* a block copolymer micelle template approach (see experimental section). After catalyst pretreatment, the Co-catalyzed growth process was performed at exactly the same temperature and CH_4 and H_2 gas flow rates as those of the SiO_2 catalyst (see experimental section). Figure 3 panels are typical SEM and AFM images of the SWNTs grown from Co catalysts with a growth duration of 20 s. SEM examinations revealed that the SWNTs catalyzed by Co catalysts exhibit a curved structure. Such a curve structure brings forth difficulty in determination of their length to some extent. However, it can be clearly discerned from the SEM image that many SWNTs are tens of micrometers in length (*e.g.,* 50 μm) and a growth velocity of ~2.5 μm/s was thus estimated, which is consistent with the previously reported values for iron group catalysts.[44−47,49] Careful AFM examinations (Figure 3b) reveal that only very few SWNTs are shorter than 1 μm. For most SWNTs, one AFM image cannot cover their two ends (the AFM images are 10 μm × 10 μm in size), indicating that the SWNTs are at least 10 micrometers in length, agreeing well with the SEM observations. These results further confirm that the slow growth velocity of the SiO_2-catalyzed SWNTs (compared to the Co-catalyzed SWNTs) originates from the intrinsic difference between the catalysts, rather than from other experimental parameters.

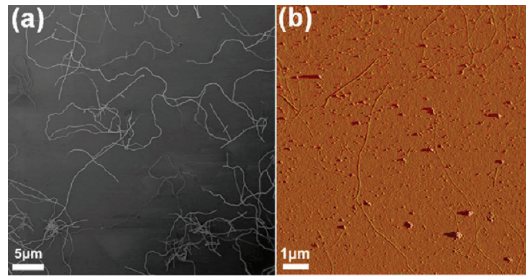

Figure 3. (a) SEM and (b) AFM images of the SWNTs grown from Co catalyst with a growth duration of 20 s.

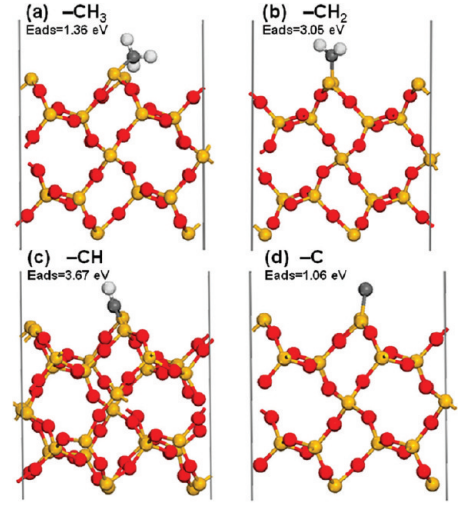

Figure 4. Optimized geometries of $-CH_x$ adsorbed on SiO_2 substrate, with Si, O, C, and H indicated as yellow, red, gray, and white spheres, respectively: (a) $-CH_3$; (b) $-CH_2$; (c) $-CH$; (d) $-C$. E_{ads} in the figure are calculated adsorption energies.

The growth velocity of the SWNTs obtained in this work is considered to be associated with several factors, including CH_4 dissociation, adsorption and diffusion of carbon species over SiO_2, and the incorporation of carbon atoms into SWNT framework. Porous materials such as SiO_2 are widely used as support materials in heterogeneous catalysis, for example, the dissociation of CH_4,[54] as also for catalytic growth of SWNTs in CVD process,[4,55] while the catalytic function of SiO_2 itself toward decomposition of hydrocarbon is very limited. Thus, we believe that CH_4 in this reaction decomposes in a pyrolysis path at high temperature. Considering the high thermal stability of CH_4[56] and that the decomposition of CH_4 is an endothermic reaction, we speculate that CH_4 decomposes in a very slow rate in the current growth process. Slow decomposition of CH_4 leads to a slow supply of carbon atoms and accordingly the slow growth velocity of SWNTs. Following the dissociation of CH_4, various C1 species (CH_x, $x = 0, 1, 2, 3$) may adsorb on SiO_2 surfaces *via* the formation of Si-CH_x, as indicated in Figure 4a−d. According to the adsorption energies we calculated (listed in each image), all C1 species can adsorb on SiO_2 surfaces with stable configurations (see optimized geometries in Figure 4). However, we noted that all the adsorption energies are lower than the bond dissociation energy of H−CH_3 (4.75 eV at the same calculation level), so we speculate that the bond dissociation of Si−CH_x may frequently occur and thus the back reaction, $CH_x + (4 - x)\,H \rightarrow CH_4$, is active, which can also slow down the growth of SWNTs.

Microscopically, the mechanism of SWNT formation starts *via* C/C coupling, and C/C chain growth can be accounted by a simple polymerization mechanism with CH_x serving as building monomers according to the Anderson−Schulz−Flory theory.[57] At the current stage,

it is not clear whether the C/C coupling is more preferable than hydrogenation on SiO_2 surfaces under our experimental conditions, which may affect the nucleation and the growth of SWNTs. Once the framework of early SWNTs forms, carbon atoms can be incorporated into the SWNT wall readily even at temperatures lower[38,55] than 900 °C in this study, since the incorporation of carbon atoms into the SWNT wall is an exothermic reaction.[38] In brief, it is reasonable to believe that the low growth velocity obtained in our work originates from several factors, such as the low decomposition rate of CH_4 on SiO_2 and the back reaction.

Further reduction in the growth time was limited because of the response limitation of the gas controller in the current work. However, it is reasonable to expect that by further optimizing the growth parameters, such as by improving the response sensitivity of gas controller (so that even shorter CH_4 feeding time can be precisely controlled), diluting the concentration of CH_4,[39] and growing at a lower temperature,[53] SWNTs with even shorter average length can be obtained.

Long Lifetime of Catalytic Activity. Another very important feature of the SiO_2 catalyst we found is its longer lifetime of catalytic activity. Renia *et al.* found that the catalytic activity lifetime of Fe catalysts for the growth of random SWNT networks is quite short, typically, less than 10 s.[44] The growth of SWNTs terminates regardless of time duration, when the reaction time exceeds 10 s, as confirmed by the same length distributions of SWNTs grown for 10 s, 30 s, 1 min, and 15 min.[44] It is generally accepted that the deactivation/poisoning of iron group catalysts is caused by the excess carbon coating during carbon decomposition in CVD process,[48] and thus several etching radicals, such as H_2O[49] or O_2,[58] are usually employed to reactivate the catalysts and prolong their catalytic lifetime.

It is interesting to find in this study that the catalytic activity lifetime of SiO_2 catalysts for the growth of random SWNT networks is far longer that 10 s, and the catalyst may keep active during the whole 20 min growth process. We examined the SWNTs obtained with further extended growth durations. Figure 5 panels are SEM images of the SWNTs with growth durations of 1 min (a), 2 min (b), 5 min (c), and 20 min (d) from SiO_2 catalyst. It is evident that the SWNTs grown for 1 min is quite short (as seen for many tips and/or ends of the SWNTs in Figure 5a) and large areas of bare substrate surface can be seen. By increasing the growth time to 2 min (Figure 5b), a relatively denser SWNT film was formed, while many ends can also be clearly discerned, indicating many short SWNTs. Further increasing the growth time to 5 min leads to the formation of a dense SWNT film where very few ends can be observed (Figure 5c). The SWNTs obtained with a 20 min growth time present as an extremely dense SWNT "mat" and the substrate surface can hardly be seen in this magnification (Figure 5d). Note that the increase of

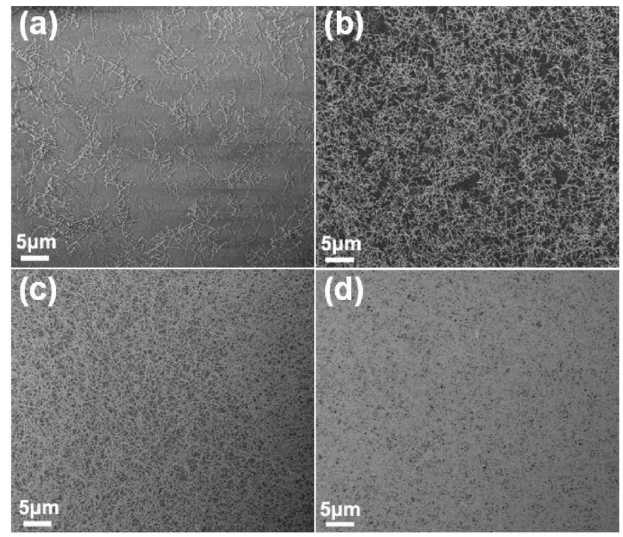

Figure 5. Representative SEM images of the SiO_2-catalyzed SWNTs with growth durations of 1 min (a), 2 min (b), 5 min (c), and 20 min (d). The SWNTs in panels a and b are relatively short, evidenced by the discernible nanotube ends. The SWNTs in panels c and d are much more densely packed, where the nanotube ends can be hardly seen in this magnification. All the SEM images were taken at a low electron acceleration voltage of 1 kV.

SWNT density may originate from either the increase of SWNT length for each SWNT or the increase of new nucleation sites. To further elucidate this point, both AFM and high-magnification SEM characterizations were performed to evaluate the length of the SWNTs for the 20 min growth sample (Figure 6). The AFM image in Figure 6a reveals that very few tips and/or ends of SWNTs can be found in a 5×5 μm^2 area. To exclude the possibility of the cross covering of SWNT ends by other SWNTs because of the high nanotube density, we performed high-magnification SEM observations as shown in Figure 6b. Careful inspections reveal that the SWNTs possess relatively diverse length distribution, where most of the SWNTs have a length in the range of $\sim 6-15$ μm. We obtained a growth velocity of 8.3 nm/s for the SiO_2-catalyzed SWNTs based on the results obtained within 1 min growth duration (Figure 2). Provided that a SWNT grows continuously with this velocity in 20 min, a tube length of ~ 10 μm would be achieved (inset of Figure 2), which is roughly consistent with the result shown in Figure 6. The aforemen-

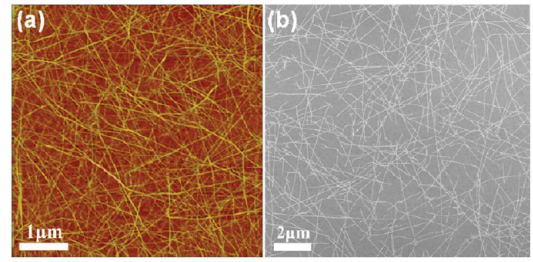

Figure 6. AFM image (a) and high-magnification SEM image (b) of the SWNTs grown for 20 min from SiO_2 catalyst, showing that most of the SWNTs are at least several micrometers in length. The SEM image was taken at 15 kV.

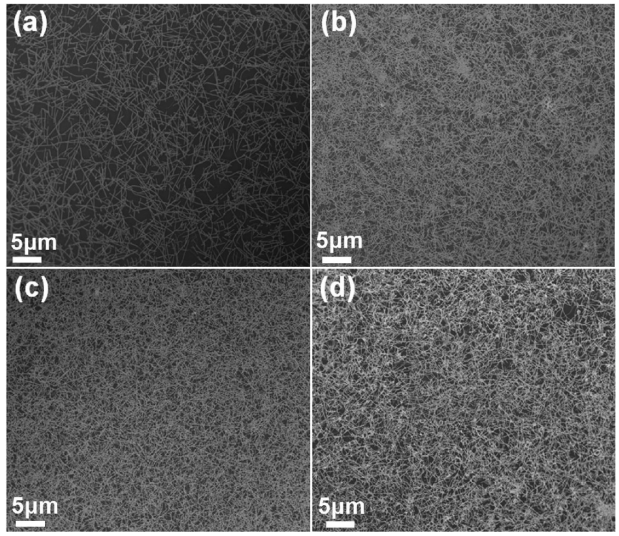

Figure 7. SEM images of the Co-catalyzed SWNTs with growth durations of 1 (a), 2 (b), 5 (c), and 20 min (d). It can be discerned from the images that the samples with growth durations of 2, 5, and 20 min possess a similar apparent SWNT density. The SEM images were taken at 1 kV.

tioned results indicate that the SiO_2 catalyst does not lose its catalytic activity in the 20 min growth process.

To make this point more solid, we also compared SiO_2 with Co catalyst for growth of SWNTs, at exactly the same reaction temperature and CH_4/H_2 flow rate, while varying time from 1 to 20 min. Upon inspection of the SEM images in Figure 7, it is evident that the SWNTs grown from Co catalyst for 1 min (Figure 7a) have a relative sparse density compared to the SWNTs grown for 2 min (Figure 7b), 5 min (Figure 7c), and 20 min (Figure 7d). However, no detectable difference in density can be found among those samples with growth time of 2, 5, and 20 min. Although it is difficult to analyze precisely the length distribution of SWNTs in Figure 7b−d due to their curving nature, long length, and high density, the apparent similar SWNT density indicates that the SWNT growth is terminated in a time scale of ~2 min for Co catalyst in this growth condition (because both the continuous growth of each SWNT and the increase of new nucleation sites would lead to the increase of apparent SWNT density). Since no etching radicals[49,58] were used in this study, it is quite possible that the short catalytic activity lifetime of Co catalyst is caused by the deactivation/poisoning due to excess carbon coating during CH_4 decomposition.[49,58] This result agrees with the short activity lifetime for Fe catalyst toward growth of random SWNT networks by Reina *et al.*[44] The sharp contrast between SiO_2 with Co catalyst in terms of catalytic activity lifetime is important toward deep understanding of the difference in growth mechanism operative in the two catalyst systems, which needs further theoretical and experimental investigations and is currently under way in our group.

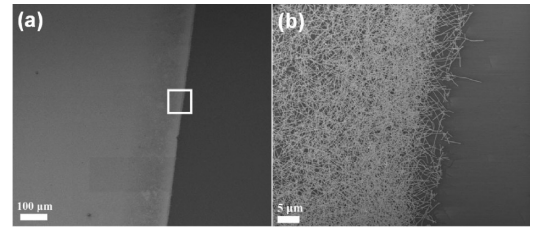

Figure 8. SEM images of the SWNTs grown from a line pattern deposited 30-nm-thick SiO_2 film, with a growth duration of 10 min. (a) Low magnification SEM image: the left side (light color) is the SiO_2 deposited area while the right side is free of SiO_2 film deposition. (b) Enlarged SEM image of the white square area in panel a showing that SWNTs are well restricted in the SiO_2 film-deposited area. The SEM images were taken at 1 kV.

Patterned Growth. Practical applications of SWNTs often require the precise positioning of SWNTs at specific regions on substrates and abundant efforts have been devoted toward both pregrowth patterning (patterning the catalyst first before SWNTs growth *via* photolithography, electron-beam lithography, or shadow masking, and thus SWNTs growth can be restricted to certain areas) and postgrowth patterning (pattering SWNTs after their growth *via* selective removal of SWNTs at certain areas by etchants) approaches to fulfill these goals.[59] The pregrowth patterning is obviously more attractive because of its simplicity, low cost, and no damage to SWNTs. Considerable efforts have been devoted to patterning growth of SWNT networks on surfaces using iron group catalysts.[59−62] However, in these previous works, severe crossing of SWNTs between patterns happened unavoidably,[59−62] and SWNTs can only be restricted in regions of hundreds of micrometers, which is caused by the rapid growth and the long length of as-grown SWNTs.[59]

On the basis of the slow growth velocity of the SiO_2-catalyzed SWNTs, we can achieve site-selective patterned growth of SWNT networks with different pattern widths by using SiO_2 catalyst and simply adjusting the growth time correspondingly, and SWNT networks can be well restricted in patterns narrower than 5 μm. As simple examples, we demonstrated the growth of SWNTs from linear patterns and grid patterns. Figure 8 shows the SWNTs grown from linear patterns with a strip-like Si wafer as a shadow mask during the SiO_2 film deposition process. The right side of Figure 8a is the sheltered area without SiO_2 film deposition. An enlarged image (Figure 8b) clearly show that dense SWNT networks were grown on the SiO_2 film-deposited area (left side), while no SWNTs can be found on the SiO_2-free area (right side). Figure 9 are SEM and AFM images of the SWNTs grown from grid patterns using tungsten or copper transmission electron microscopy (TEM) grids as shadow masks. One can see that SWNT networks were grown in large area uniform patterns (Figure 9a) and can be well restricted within patterns with a width <5 μm (Figure 9b−d). Careful AFM characterization confirmed that SWNTs are well restricted in the

SiO_2 film-deposited area (Figure 9e), while no SWNTs or NPs were found in the areas without SiO_2 film deposition (Figure 9f). These results demonstrate that these SWNTs catalyzed by SiO_2 can be well confined into a narrower region and no distinct crossing is observed at the interface area, which shows an obviously better pattern precision compared to the previous approaches using iron group catalysts.[59−62] The better pattern precision in the current study is beneficial from the slow growth velocity of SWNTs, which leads to a more precise control over the growth process. This point is evidenced by the fact that further increasing the growth time from 2 to 20 min will lead to a crossover of the SWNTs between the patterns because of their extended length (see Supporting Information, Figure S4). These preliminary results on patterned growth of SWNTs suggest that catalysts can be easily and efficiently confined in small areas during film deposition process, and more importantly, the SWNTs can be selectively grown at narrow defined locations in a reproducible and highly manufacturable manner, which is important for the effective integration of SWNTs into device frameworks. Precise location−controlled growth is one of the major concerns on applications of SWNTs in electronic devices, and the abstaining of metal species can enhance the compatibility with silicon semiconductor processing and improve the reliability of device performance. The metal-free SWNTs obtained, combined with the good position controllability, are highly desirable for fabrication of SWNT-based thin film devices.

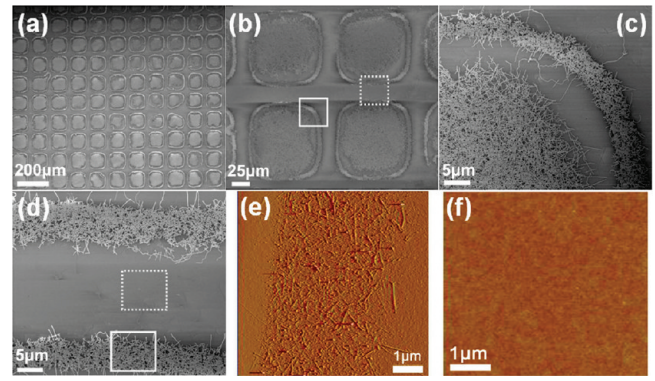

Figure 9. SEM images of the SWNTs grown from patterns using tungsten TEM grid as a shadow mask, with a growth duration of 2 min. (a and b) Low- and high-magnification images of the pattern images. (c and d) SWNTs grown from the solid and dotted square areas in panel b, showing well-positioning controllability. (e and f) AFM images of the solid and dotted square areas in panel d, showing that the SWNTs were selectively grown on SiO_2 film-deposited area (e). No SWNTs or catalyst NPs can be found in SiO_2 film-free area (f). The SEM images were taken at 1 kV.

CONCLUSIONS

Short SWNTs with an average length of 149, 342, and 483 nm are selectively obtained *via* a direct metal-catalyst-free CVD growth process, where SiO_2 serves as the catalyst. A very slow growth velocity of 8.3 nm/s was obtained for the SiO_2-catalyzed growth of SWNTs, about 300 times slower than that of the SWNTs catalyzed by the commonly used iron group catalysts. The slow growth velocity facilitates the length-controlled growth of SWNTs, and SWNTs as short as ~20 nm were directly grown. Furthermore, it was found that the SiO_2-based catalyst keeps active during the whole 20 min growth process, as confirmed by the continuous increase of the average SWNT length with prolonged growth time. In a sharp contrast, comparative studies reveal that Co catalyst is easily deactivated in a short time within 2 min, possibly due to the catalyst poisoning. Taking advantages of the slow growth velocity, confined growth of SWNT patterns with a width <5 μm was achieved. Such metal impurity-free, length-sorted, and precisely confined SWNTs is desirable for various applications, such as fabrication of electronic devices. In addition, the ultralow growth velocity of the SiO_2-catalyzed SWNTs and the long catalytic lifetime of the SiO_2 catalyst may indicate a unique growth mechanism. A comprehensive understanding of the mechanism operative in these processes will be helpful for the fine structure control of SWNTs; further investigations are under way.

EXPERIMENTAL AND THEORETICAL SECTION

Metal-Catalyst-Free Growth of SWNTs. The metal-catalyst-free CVD process used is similar to our previous communication with some appropriate improvements.[41] In a typical experimental run, a 30-nm-thick SiO_2 film deposited SiO_2/Si (1-μm-thick thermally grown SiO_2 layer) wafer was employed as substrate. The SiO_2 film deposition was conducted in a Gatan model 682 precision etching coating system using single crystal SiO_2 as target material (99.99% purity, purchased from Hefei Kejing Materials Technology Co., Ltd., China). The SiO_2 film deposited SiO_2/Si wafers were first loaded into a small quartz tube (diameter, 10 mm; length, 30 cm).[63,64] This small tube was then inserted into a reaction quartz tube (diameter, 25 mm; length, 120 cm), which was fixed in a Lindberg/BlueM tube furnace. The substrates were first annealed in N_2 + O_2 gas mixture (4:1, v:v, total flow rate 200 sccm) at 850 °C for 10 min. Ar (1000 sccm) was then introduced to exhaust O_2 for 8 min, and the furnace temperature was increased to 900 °C during this period. Then 500 sccm CH_4 and 500 sccm H_2 were introduced into the quartz tube to initiate the reaction. All the gases were controlled by mass flow controllers (MFCs). The growth durations varied from 20 s to 20 min. After growth, the furnace was cooled naturally down to room temperature under the protection of Ar + H_2 gas mixture (500 sccm + 200 sccm). To best avoid the influence of residual CH_4 on the evaluation of the growth velocity of SWNTs with time periods of 20, 40, and 60 s, two means were applied: (i) flushing the residual CH_4 gas with large flow rates of Ar + H_2 gas mixture (1000 sccm + 500 sccm), and (ii) pulling out the reaction tube from high temperature area just after switching off the CH_4 gas.

Co-catalyzed Growth of SWNTs. The Co catalyst NPs were synthesized *via* a block copolymer micelle template approach.[62,65,66] We employed polystyrene-*b*-poly(4-vinyl pyridine) (denoted as PS-*b*-P4 VP hereafter; M_n-PS-*b*-P4 VP, 40000-*b*-5600; polydispersity index (PDI), 1.09; purchased from Polymer Source) for Co NP synthesis. In a typical experiment, PS-*b*-P4 VP (24.5 mg) was added into toluene (25 mL) and stirred for 5 h at room tempera-

ture to dissolve the polymer to form a 0.11 wt % solution. Cobalt(II) acetate tetrahydrate ($Co(CH_3CO_2)_2 \cdot 4H_2O$) (2.1 mg) was then added into the polymer solution and stirred for another 48 h at room temperature. During this stirring process, the complexation of transition metal Co with that of pyridine group (the molar ratio of Co to pyridine unit was 0.29) generated spherical micelles in toluene whose cores consist of cobalt-complexed P4 VP blocks encapsulated by PS chains.[65] The as-formed Co-bearing solution micelles were spin-coated onto SiO_2/Si wafers at 3000 rpm for 1 min (Chemat Technology, Spin-Coater, KW-4A) and followed by oxygen plasma treatment to remove the polymers for 10 min (Plasma Cleaner, PDC-32G). The plasma treated substrates were then subjected into the tube furnace with the same configurations as described for metal-catalyst-free CVD process. Dedicated, new quartz tubes were employed for the two catalyst systems to avoid any possible catalyst cross-contamination. Co catalyst was first annealed at 700 °C for 1 min in $N_2 + O_2$ (4:1, v:v, total flow rate 200 sccm). Ar (1000 sccm) was introduced to exhaust O_2 for 8 min and the furnace ramped to 900 °C in this duration. After the reduction of Co catalyst at 900 °C for 3 min in Ar + H_2 (500 sccm + 200 sccm), 500 sccm of CH_4 together with 500 sccm of H_2 was introduced to initiate SWNT growth for 20 s to 20 min. After growth, the tube furnace was cooled down to room temperature under Ar + H_2 (500 sccm + 200 sccm) gas mixture.

SWNT Characterizations. The as-grown SWNTs were extensively characterized by using atomic force microscopy (AFM, multimode NanoScope IIIa, Vecco, operated in tapping mode), scanning electron microscopy (SEM, Nova NanoSEM 430, 1 kV and 15 kV), and Raman spectroscopy (Jobin Yvon HR800, with 632.8 nm He−Ne laser and laser spot size of ~1 μm^2).

Theoretical Calculations. Spin-polarized density functional theory (DFT) calculations were carried out to investigate the adsorption geometries of $-CH_x$ over SiO_2 substrates. The SiO_2 substrate was described by the majority surface of (1 −1 0) using a 2 × 2 slab model (9.8 Å × 10.8 Å), with the vacuum thickness being more than 15 Å. All geometry optimizations and single point energies were carried out using the atomic-centered basic functions implemented with the Dmol3 package.[67] Exchange and correlation were treated in the generalized gradient approximation (GGA) of Perdew−Burke−Ernzerhof (PBE).[68] Due to the large size of the slab model, the k-point is only set as 1 × 1 × 1. During the optimizations, the criteria for energy and displacement convergence were set as 10^{-5} Hartree and 5 × 10^{-3} Å. With higher convergence criteria, the changes of calculated adsorption energies were less than 0.02 eV, which is good enough to describe the difference (>1.5 eV as indicated in the text) between the adsorption energies of $-CH_x$ over SiO_2 and the bond dissociation energy of CH_4.

Acknowledgment. This work was financially supported by MOST of China (Nos. 2006CB932701 and 2008DFA51400), NSFC (Nos. 90606008, 50702063, and 50921004), and CAS (No. KJCX2-YW-M01).

Supporting Information Available: AFM characterization of Co NPs, Raman spectrum of Co-catalyzed SWNTs, schematic illustration of the grid masks used for patterning growth, SEM images of the SWNTs grown from grid patterns with growth time of 10 min, and SEM image comparison of SWNTs at different electron acceleration voltages. This material is available free of charge *via* the Internet at http://pubs.acs.org.

REFERENCES AND NOTES

1. Jorio, A.; Dresselhaus, G.; Dresselhaus, M. S. *Carbon Nanotubes*; Topics in Applied Physics, Vol 111; Springer-Verlag: Berlin/Heidelberg, 2008.
2. Engel, M.; Small, J. P.; Steiner, M.; Freitag, M.; Green, A. A.; Hersam, M. C.; Avouris, P. Thin Film Nanotube Transistors Based on Self-Assembled, Aligned, Semiconducting Carbon Nanotube Arrays. *ACS Nano* **2008**, *2*, 2445–2452.
3. Martel, R. Sorting Carbon Nanotubes for Electronics. *ACS Nano* **2008**, *2*, 2195–2199.
4. Bachilo, S. M.; Balzano, L.; Herrera, J. E.; Pompeo, F.; Resasco, D. E.; Weisman, R. B. Narrow (*n*,*m*)-Distribution of Single-Walled Carbon Nanotubes Grown Using a Solid Supported Catalyst. *J. Am. Chem. Soc.* **2003**, *125*, 11186–11187.
5. Smalley, R. E.; Li, Y. B.; Moore, V. C.; Price, B. K.; Colorado, R.; Schmidt, H. K.; Hauge, R. H.; Barron, A. R.; Tour, J. M. Single Wall Carbon Nanotube Amplification: En Route to a Type-Specific Growth Mechanism. *J. Am. Chem. Soc.* **2006**, *128*, 15824–15829.
6. Chen, Y.; Wei, L.; Wang, B.; Lim, S. Y.; Ciuparu, D.; Zheng, M.; Chen, J.; Zoican, C.; Yang, Y. H.; Haller, G. L.; Pfefferle, L. D. Low-Defect, Purified, Narrowly (*n*,*m*)-Dispersed Single-Walled Carbon Nanotubes Grown from Cobalt-Incorporated MCM-41. *ACS Nano* **2007**, *1*, 327–336.
7. Qu, L. T.; Du, F.; Dai, L. M. Preferential Syntheses of Semiconducting Vertically Aligned Single-Walled Carbon Nanotubes for Direct Use in FETs. *Nano Lett.* **2008**, *8*, 2682–2687.
8. Ding, L.; Tselev, A.; Wang, J. Y.; Yuan, D. N.; Chu, H. B.; McNicholas, T. P.; Li, Y.; Liu, J. Selective Growth of Well-Aligned Semiconducting Single-Walled Carbon Nanotubes. *Nano Lett.* **2009**, *9*, 800–805.
9. Zheng, M.; Jagota, A.; Semke, E. D.; Diner, B. A.; Mclean, R. S.; Lustig, S. R.; Richardson, R. E.; Tassi, N. G. DNA-Assisted Dispersion and Separation of Carbon Nanotubes. *Nat. Mater.* **2003**, *2*, 338–342.
10. Zhang, G. Y.; Qi, P. F.; Wang, X. R.; Lu, Y. R.; Li, X. L.; Tu, R.; Bangsaruntip, S.; Mann, D.; Zhang, L.; Dai, H. J. Selective Etching of Metallic Carbon Nanotubes by Gas-Phase Reaction. *Science* **2006**, *314*, 974–977.
11. Arnold, M. S.; Green, A. A.; Hulvat, J. F.; Stupp, S. I.; Hersam, M. C. Sorting Carbon Nanotubes by Electronic Structure Using Density Differentiation. *Nat. Nanotechnol.* **2006**, *1*, 60–65.
12. Huang, X. Y.; McLean, R. S.; Zheng, M. High-Resolution Length Sorting and Purification of DNA-Wrapped Carbon Nanotubes by Size-Exclusion Chromatography. *Anal. Chem.* **2005**, *77*, 6225–6228.
13. Mingo, N.; Broido, D. A. Length Dependence of Carbon Nanotube Thermal Conductivity and the Problem of Long Waves. *Nano Lett.* **2005**, *5*, 1221–1225.
14. Simien, D.; Fagan, J. A.; Luo, W.; Douglas, J. F.; Migler, K.; Obrzut, J. Influence of Nanotube Length on the Optical and Conductivity Properties of Thin Single-Wall Carbon Nanotube Networks. *ACS Nano* **2008**, *2*, 1879–1884.
15. Onoa, G. B.; O'Reilly, T. B.; Walsh, M. E.; Smith, H. I. Bulk Production of Singly Dispersed Carbon Nanotubes with Prescribed Lengths. *Nanotechnology* **2005**, *16*, 2799–2803.
16. Javey, A.; Guo, J.; Paulsson, M.; Wang, Q.; Mann, D.; Lundstrom, M.; Dai, H. J. High-Field Quasiballistic Transport in Short Carbon Nanotubes. *Phys. Rev. Lett.* **2004**, *92*, 106804–106807.
17. Hod, O.; Scuseria, G. E. Half-Metallic-Zigzag Carbon Nanotube Dots. *ACS Nano* **2008**, *2*, 2243–2249.
18. Venema, L. C.; Wildoer, J. W. G.; Janssen, J. W.; Tans, S. J.; Tuinstra, H. L. J. T.; Kouwenhoven, L. P.; Dekker, C. Imaging Electron Wave Functions of Quantized Energy Levels in Carbon Nanotubes. *Science* **1999**, *283*, 52–55.
19. Lu, W.; Xiong, Y.; Chen, L. Length-Dependent Dielectric Polarization in Metallic Single-Walled Carbon Nanotubes. *J. Phys. Chem. C* **2009**, *113*, 10337–10340.
20. Wang, Z. L.; Tang, D. W.; Li, X. B.; Zheng, X. H.; Zhang, W. G.; Zheng, L. X.; Zhu, Y. T. T.; Jin, A. Z.; Yang, H. F.; Gu, C. Z. Length-Dependent Thermal Conductivity of an Individual Single-Wall Carbon Nanotube. *Appl. Phys. Lett.* **2007**, *91*, 123119–123121.
21. Liu, Z.; Tabakman, S.; Welsher, K.; Dai, H. Carbon Nanotubes in Biology and Medicine: *In Vitro* and *in Vivo* Detection, Imaging, and Drug Delivery. *Nano Res.* **2009**, *2*, 85–120.
22. Sun, X.; Zaric, S.; Daranciang, D.; Welsher, K.; Lu, Y.; Li, X.; Dai, H. Optical Properties of Ultrashort Semiconducting Single-Walled Carbon Nanotube Capsules down to Sub-10 nm. *J. Am. Chem. Soc.* **2008**, *130*, 6551–6555.

23. Hafner, J. H.; Cheung, C. L.; Oosterkamp, T. H.; Lieber, C. M. High-Yield Assembly of Individual Single-Walled Carbon Nanotube Tips for Scanning Probe Microscopies. *J. Phys. Chem. B* **2001**, *105*, 743–746.
24. Hafner, J. H.; Cheung, C. L.; Lieber, C. M. Direct Growth of Single-Walled Carbon Nanotube Scanning Probe Microscopy Tips. *J. Am. Chem. Soc.* **1999**, *121*, 9750–9751.
25. Chen, W.; Fan, Z. L.; Pan, X. L.; Bao, X. H. Effect of Confinement in Carbon Nanotubes on the Activity of Fischer−Tropsch Iron Catalyst. *J. Am. Chem. Soc.* **2008**, *130*, 9414–9419.
26. Ziegler, K. J.; Gu, Z. N.; Shaver, J.; Chen, Z. Y.; Flor, E. L.; Schmidt, D. J.; Chan, C.; Hauge, R. H.; Smalley, R. E. Cutting Single-Walled Carbon Nanotubes. *Nanotechnology* **2005**, *16*, S539–S544.
27. Wang, S. R.; Liang, Z. Y.; Wang, B.; Zhang, C.; Rahman, Z. Precise Cutting of Single-Walled Carbon Nanotubes. *Nanotechnology* **2007**, *18*, 055301−055306.
28. Chen, J.; Dyer, M. J.; Yu, M. F. Cyclodextrin-Mediated Soft Cutting of Single-Walled Carbon Nanotubes. *J. Am. Chem. Soc.* **2001**, *123*, 6201–6202.
29. Stepanek, I.; Maurin, G.; Bernier, P.; Gavillet, J.; Loiseau, A.; Edwards, R.; Jaschinski, O. Nano-Mechanical Cutting and Opening of Single Wall Carbon Nanotubes. *Chem. Phys. Lett.* **2000**, *331*, 125–131.
30. Pierard, N.; Fonseca, A.; Colomer, J. F.; Bossuot, C.; Benoit, J. M.; Van Tendeloo, G.; Pirard, J. P.; Nagy, J. B. Ball Milling Effect on the Structure of Single-Wall Carbon Nanotubes. *Carbon* **2004**, *42*, 1691–1697.
31. Fagan, J. A.; Becker, M. L.; Chun, J.; Hobbie, E. K. Length Fractionation of Carbon Nanotubes Using Centrifugation. *Adv. Mater.* **2008**, *20*, 1609–1613.
32. Liu, J.; Rinzler, A. G.; Dai, H. J.; Hafner, J. H.; Bradley, R. K.; Boul, P. J.; Lu, A.; Iverson, T.; Shelimov, K.; Huffman, C. B.; *et al*. Fullerene Pipes. *Science* **1998**, *280*, 1253–1256.
33. Gu, Z.; Peng, H.; Hauge, R. H.; Smalley, R. E.; Margrave, J. L. Cutting Single-Wall Carbon Nanotubes through Fluorination. *Nano Lett.* **2002**, *2*, 1009–1013.
34. Chen, Z. Y.; Kobashi, K.; Rauwald, U.; Booker, R.; Fan, H.; Hwang, W. F.; Tour, J. M. Soluble Ultrashort Single-Walled Carbon Nanotubes. *J. Am. Chem. Soc.* **2006**, *128*, 10568–10571.
35. O'Connell, M. J.; Bachilo, S. M.; Huffman, C. B.; Moore, V. C.; Strano, M. S.; Haroz, E. H.; Rialon, K. L.; Boul, P. J.; Noon, W. H.; Kittrell, C.; *et al*. Band Gap Fluorescence from Individual Single-Walled Carbon Nanotubes. *Science* **2002**, *297*, 593–596.
36. Moore, V. C.; Strano, M. S.; Haroz, E. H.; Hauge, R. H.; Smalley, R. E.; Schmidt, J.; Talmon, Y. Individually Suspended Single-Walled Carbon Nanotubes in Various Surfactants. *Nano Lett.* **2003**, *3*, 1379–1382.
37. Wei, Z.; Chen, Y.; Liu, Z. F. Preparation of Short Single Walled Carbon Nanotubes by CVD Growth and by Chemical Oxidation. *Acta Phys., Chim. Sin.* **2001**, *17*, 687–691.
38. Mora, E.; Pigos, J. M.; Ding, F.; Yakobson, B. I.; Harutyunyan, A. R. Low-Temperature Single-Wall Carbon Nanotubes Synthesis: Feedstock Decomposition Limited Growth. *J. Am. Chem. Soc.* **2008**, *130*, 11840–11841.
39. Hafner, J. H.; Bronikowski, M. J.; Azamian, B. R.; Nikolaev, P.; Rinzler, A. G.; Colbert, D. T.; Smith, K. A.; Smalley, R. E. Catalytic Growth of Single-Wall Carbon Nanotubes from Metal Particles. *Chem. Phys. Lett.* **1998**, *296*, 195–202.
40. Ding, F.; Rosen, A.; Bolton, K. Dependence of SWNT Growth Mechanism on Temperature and Catalyst Particle Size: Bulk *versus* Surface Diffusion. *Carbon* **2005**, *43*, 2215–2217.
41. Liu, B. L.; Ren, W. C.; Gao, L. B.; Li, S. S.; Pei, S. F.; Liu, C.; Jiang, C. B.; Cheng, H. M. Metal-Catalyst-Free Growth of Single-Walled Carbon Nanotubes. *J. Am. Chem. Soc.* **2009**, *131*, 2082–2083.
42. Hirsch, A. Growth of Single-Walled Carbon Nanotubes Without A Metal Catalyst—A Surprising Discovery. *Angew. Chem., Int. Ed.* **2009**, *48*, 5403–5404.
43. Huang, S. M.; Cai, Q. R.; Chen, J. Y.; Qian, Y.; Zhang, L. J. Metal-Catalyst-Free Growth of Single-Walled Carbon Nanotubes on Substrates. *J. Am. Chem. Soc.* **2009**, *131*, 2094–2095.
44. Reina, A.; Hofmann, M.; Zhu, D.; Kong, J. Growth Mechanism of Long and Horizontally Aligned Carbon Nanotubes by Chemical Vapor Deposition. *J. Phys. Chem. C* **2007**, *111*, 7292–7297.
45. Huang, S. M.; Woodson, M.; Smalley, R.; Liu, J. Growth Mechanism of Oriented Long Single Walled Carbon Nanotubes Using "Fast-Heating" Chemical Vapor Deposition Process. *Nano Lett.* **2004**, *4*, 1025–1028.
46. Yao, Y. G.; Liu, R.; Zhang, J.; Jiao, L. Y.; Liu, Z. F. Raman Spectral Measuring of the Growth Rate of Individual Single-Walled Carbon Nanotubes. *J. Phys. Chem. C* **2007**, *111*, 8407–8409.
47. Jin, Z.; Chu, H. B.; Wang, J. Y.; Hong, J. X.; Tan, W. C.; Li, Y. Ultralow Feeding Gas Flow Guiding Growth of Large-Scale Horizontally Aligned Single-Walled Carbon Nanotube Arrays. *Nano Lett.* **2007**, *7*, 2073–2079.
48. Crouse, C. A.; Maruyama, B.; Colorado, R.; Back, T.; Barron, A. R. Growth, New Growth, and Amplification of Carbon Nanotubes as a Function of Catalyst Composition. *J. Am. Chem. Soc.* **2008**, *130*, 7946–7954.
49. Hata, K.; Futaba, D. N.; Mizuno, K.; Namai, T.; Yumura, M.; Iijima, S. Water-Assisted Highly Efficient Synthesis of Impurity-Free Single-Walled Carbon Nanotubes. *Science* **2004**, *306*, 1362–1364.
50. Huang, S. M.; Cai, X. Y.; Liu, J. Growth of Millimeter-Long and Horizontally Aligned Single-Walled Carbon Nanotubes on Flat Substrates. *J. Am. Chem. Soc.* **2003**, *125*, 5636–5637.
51. Huang, L. M.; Cui, X. D.; White, B.; O'Brien, S. P. Long and Oriented Single-Walled Carbon Nanotubes Grown by Ethanol Chemical Vapor Deposition. *J. Phys. Chem. B* **2004**, *108*, 16451–16456.
52. Zheng, L. X.; O'Connell, M. J.; Doorn, S. K.; Liao, X. Z.; Zhao, Y. H.; Akhadov, E. A.; Hoffbauer, M. A.; Roop, B. J.; Jia, Q. X.; Dye, R. C.; *et al*. Ultralong Single-Wall Carbon Nanotubes. *Nat. Mater.* **2004**, *3*, 673–676.
53. Zheng, L. X.; Satishkumar, B. C.; Gao, P. Q.; Zhang, Q. Kinetics Studies of Ultralong Single-Walled Carbon Nanotubes. *J. Phys. Chem. C* **2009**, *113*, 10896–10900.
54. Wang, H. Y.; Au, C. T. Carbon Dioxide Reforming of Methane to Syngas over SiO_2-Supported Rhodium Catalysts. *Appl. Catal., A* **1997**, *155*, 239–252.
55. Maruyama, S.; Kojima, R.; Miyauchi, Y.; Chiashi, S.; Kohno, M. Low-Temperature Synthesis of High-Purity Single-Walled Carbon Nanotubes from Alcohol. *Chem. Phys. Lett.* **2002**, *360*, 229–234.
56. Khan, M. S.; Crynes, B. L. Survey of Recent Methane Pyrolysis Literature—A Survey of Methane Pyrolysis Data Is Presented and Discussed. *Ind. Eng. Chem.* **1970**, *62*, 54–59.
57. Van der Laan, G. P.; Beenackers, A. A. C. M. Kinetics and Selectivity of the Fischer−Tropsch Synthesis: A Literature Review. *Cat. Rev.-Sci. Eng.* **1999**, *41*, 255–318.
58. Zhang, G. Y.; Mann, D.; Zhang, L.; Javey, A.; Li, Y. M.; Yenilmez, E.; Wang, Q.; McVittie, J. P.; Nishi, Y.; Gibbons, J.; Dai, H. J. Ultra-High-Yield Growth of Vertical Single-Walled Carbon Nanotubes: Hidden Roles of Hydrogen and Oxygen. *Proc. Natl. Acad. Sci. U.S.A.* **2005**, *102*, 16141–16145.
59. Edgeworth, J. P.; Wilson, N. R.; Macpherson, J. V. Controlled Growth and Characterization of Two-Dimensional Single-Walled Carbon-Nanotube Networks for Electrical Applications. *Small* **2007**, *3*, 860–870.
60. Lu, J. Q.; Moll, N.; Fu, Q.; Liu, J. Iron Nanoparticles Derived from Iron-Complexed Polymethylglutarimide to Produce High-Quality Lithographically Defined Single-Walled Carbon Nanotubes. *Chem. Mater.* **2005**, *17*, 2227–2231.
61. Ding, L.; Zhou, W. W.; Chu, H. B.; Jin, Z.; Zhang, Y.; Li, Y. Direct Preparation and Patterning of Iron Oxide Nanoparticles *via* Microcontact Printing on Silicon Wafers for the Growth of Single-Walled Carbon Nanotubes. *Chem. Mater.* **2006**, *18*, 4109–4114.

62. Lu, J.; Yi, S. S.; Kopley, T.; Qian, C.; Liu, J.; Gulari, E. Fabrication of Ordered Catalytically Active Nanoparticles Derived from Block Copolymer Micelle Templates for Controllable Synthesis of Single-Walled Carbon Nanotubes. *J. Phys. Chem. B* **2006**, *110*, 6655–6660.
63. Hong, B. H.; Lee, J. Y.; Beetz, T.; Zhu, Y. M.; Kim, P.; Kim, K. S. Quasi-continuous Growth of Ultralong Carbon Nanotube Arrays. *J. Am. Chem. Soc.* **2005**, *127*, 15336–15337.
64. Liu, B. L.; Ren, W. C.; Gao, L. B.; Li, S. S.; Liu, Q. F.; Jiang, C. B.; Cheng, H. M. Manganese-Catalyzed Surface Growth of Single-Walled Carbon Nanotubes with High Efficiency. *J. Phys. Chem. C* **2008**, *112*, 19231–19235.
65. Lu, J.; Kopley, T.; Dutton, D.; Liu, J.; Qian, C.; Son, H.; Dresselhaus, M.; Kong, J. Generating Suspended Single-Walled Carbon Nanotubes Across a Large Surface Area *via* Patterning Self-Assembled Catalyst-Containing Block Copolymer Thin Films. *J. Phys. Chem. B* **2006**, *110*, 10585–10589.
66. Bhaviripudi, S.; Reina, A.; Qi, J. F.; Kong, J.; Belcher, A. M. Block-Copolymer Assisted Synthesis of Arrays of Metal Nanoparticles and Their Catalytic Activities for the Growth of SWNTs. *Nanotechnology* **2006**, *17*, 5080–5086.
67. Delley, B. From Molecules to Solids with the DMol(3) Approach. *J. Chem. Phys.* **2000**, *113*, 7756–7764.
68. Perdew, J. P.; Burke, K.; Ernzerhof, M. Generalized Gradient Approximation Made Simple. *Phys. Rev. Lett.* **1996**, *77*, 3865–3868.